

## **Electronic Supplementary Information**

**Synthesis, characterization, luminescence properties and deciphering the role of terpyridyl-imidazole based ligand on dissimilar luminescence sensitization of ternary lanthanide(III) tris-( $\beta$ -diketonate) complexes**

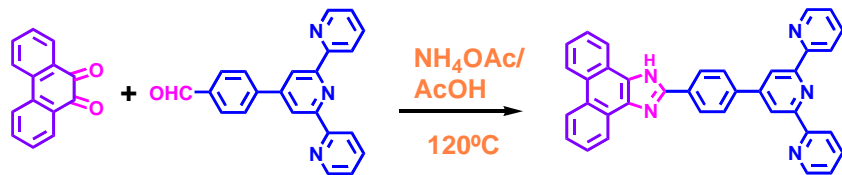
**Toushique Ahmed<sup>a</sup>, Amit Chakraborty<sup>a</sup>, Animesh Paul<sup>a</sup>, and Sujoy Baitalik<sup>a\*</sup>**

<sup>a</sup>Inorganic Chemistry Section, Department of Chemistry, Jadavpur University  
Kolkata 700032, India

## Experimental Details

### Synthesis of the ligand (tpy-HImdzphen)

The ligand was synthesized by following our reported literature procedure.<sup>35</sup> A mixture of 4'-(*p*-formylphenyl)-2,2':6',2''-terpyridine (tpy-PhCHO) (337 mg, 1.0 mmol), 9,10-phenanthrenedione (230 mg, 1.1 mmol), and ammonium acetate (1.6 g, 20 mmol) is refluxed in acetic acid and produces a pale-yellow solution which upon pouring into ice-water mixture, produces pale-yellow solid. The solid is collected by filtration, washed several times with water and upon recrystallization from chloroform-methanol (1:1) mixture produces a light yellow crystalline solid. (370 mg, 0.70 mmol, yield 70%). <sup>1</sup>H NMR (DMSO-*d*<sub>6</sub>, 500 MHz): δ = 13.60 (s, 1H, NH(imidazole), 8.86 (d, 2H, *J* = 8.5 Hz, H9), 8.82 (s, 2H, H39), 8.79 (d, 2H, *J* = 4.0 Hz, H6), 8.69 (d, 2H, *J* = 8.0 Hz, H3), 8.60 (d, 2H, *J* = 8.0 Hz, H12), 8.53 (d, 2H, *J* = 8.0 Hz, H8), 8.20 (d, 2H, *J* = 8.5 Hz, H7), 8.05 (t, 2H, *J* = 7.5 Hz, H4), 7.75 (t, 2H, *J* = 7.5 Hz, H11), 7.65 (t, 2H, *J* = 7.7 Hz, H10), 7.54 (t, 2H, *J* = 6.0 Hz, H5). ESI-MS: m/z 525.51 ([tpy-HImdzphen+H]<sup>+</sup>). Elemental analysis: Anal. Calcd for C<sub>36</sub>H<sub>23</sub>N<sub>5</sub>: C, 82.26; H, 4.41; N, 13.32. Found: C, 82.18; H, 4.44; N, 13.29.



**Scheme S1.** Synthesis of the ligand (tpy-HImdzphen).

### Synthesis of Ln(tta)<sub>3</sub>(H<sub>2</sub>O)<sub>2</sub>

All the four lanthanide precursors of the type, Ln(tta)<sub>3</sub>(H<sub>2</sub>O)<sub>2</sub>, Ln<sup>III</sup>= La<sup>III</sup>, Eu<sup>III</sup>, Sm<sup>III</sup> and Tb<sup>III</sup> are synthesized by following the reported literature procedure.<sup>49</sup> 2-theonyltrifluoroacetone (333 mg, 1.5mM) is dissolved in ethanol-water mixture (1:1, v/v) and kept for a few minutes after adding 1.5 mM aqueous solution of NaOH. LnCl<sub>3</sub>·xH<sub>2</sub>O (x=6 or 7) is then added to the mixture and stirred for 2h at 60°C. White crystalline product was found which was then filtered and dried in a vacuum desiccator for 2d.

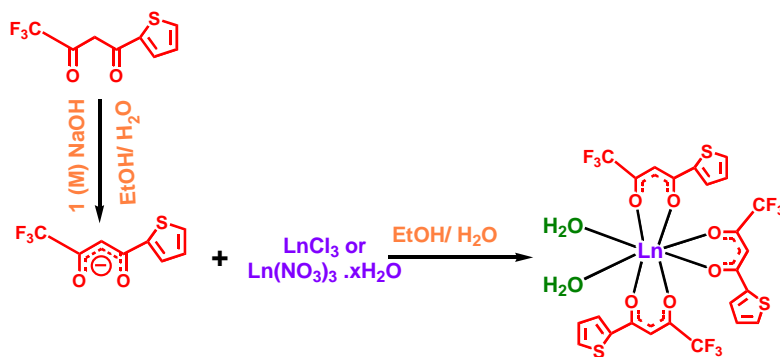
**La(tta)<sub>3</sub>(H<sub>2</sub>O)<sub>2</sub>** LaCl<sub>3</sub>·7H<sub>2</sub>O (186 mg, 0.5 mmol). Yield 235 mg (28 %). FT-IR:  $\nu$  (in cm<sup>-1</sup>) = 1610, 3360. Anal. Calcd for C<sub>24</sub>H<sub>16</sub>F<sub>9</sub>S<sub>3</sub>O<sub>8</sub>La: C, 34.38; H, 1.92. Found: C, 34.26; H, 1.86. <sup>1</sup>H

NMR (DMSO-*d*<sub>6</sub>, 400 MHz, δ/ppm): 8.02 (d, 3H, H<sub>2</sub>; *J* = 8.00 Hz), 7.97 (d, 3H, H<sub>4</sub>; *J* = 8.00 Hz), 7.25 (t, 3H, H<sub>3</sub>; *J* = 4.36 Hz), 6.40 (s, 3H, H<sub>1</sub> methine).

**Eu(tta)<sub>3</sub>(H<sub>2</sub>O)<sub>2</sub>** EuCl<sub>3</sub>·6H<sub>2</sub>O (183 mg, 0.5 mmol). Yield 252 mg (30 %). FT-IR: ν (in cm<sup>-1</sup>) = 1603, 3351. Anal. Calcd for C<sub>24</sub>H<sub>16</sub>F<sub>9</sub>S<sub>3</sub>O<sub>8</sub>Eu: C, 33.85; H, 1.89. Found: C, 33.78; H, 1.84. <sup>1</sup>H NMR (DMSO-*d*<sub>6</sub>, 400 MHz, δ/ppm): 8.00 (d, 3H, H<sub>2</sub>; *J* = 4.80 Hz), 7.95 (d, 3H, H<sub>4</sub>; *J* = 3.92 Hz), 7.24 (t, 3H, H<sub>3</sub>; *J* = 4.84 Hz), 1.10 (s, 3H, H<sub>1</sub> methine).

**Sm(tta)<sub>3</sub>(H<sub>2</sub>O)<sub>2</sub>** SmCl<sub>3</sub>·6H<sub>2</sub>O (182 mg, 0.5 mmol). Yield 216 mg (25 %). FT-IR: ν (in cm<sup>-1</sup>) = 1602, 3353. Anal. Calcd for C<sub>24</sub>H<sub>16</sub>F<sub>9</sub>S<sub>3</sub>O<sub>8</sub>Sm: C, 33.92; H, 1.90; Found: C, 33.86; H, 1.83. <sup>1</sup>H NMR (DMSO-*d*<sub>6</sub>, 400 MHz, δ/ppm): 8.13 (s, 3H, H<sub>1</sub> methine), 7.55 (s, 3H, H<sub>2</sub>), 7.32 (s, 3H, H<sub>3</sub>), 7.21 (t, 3H, H<sub>4</sub>; *J* = 4.56 Hz).

**Tb(tta)<sub>3</sub>(H<sub>2</sub>O)<sub>2</sub>** TbCl<sub>3</sub>·6H<sub>2</sub>O (187 mg, 0.5 mmol). Yield 227 mg (26 %). FT-IR: ν (in cm<sup>-1</sup>) = 1601, 3400. Anal. Calcd for C<sub>24</sub>H<sub>16</sub>F<sub>9</sub>S<sub>3</sub>O<sub>8</sub>Tb: C, 33.58; H, 1.88. Found: C, 33.55; H, 1.81. <sup>1</sup>H NMR (DMSO-*d*<sub>6</sub>, 400 MHz, δ/ppm): 95.97 (s, 3H, H<sub>1</sub> methine), 29.14 (s, 3H, H<sub>2</sub>), 12.22 (s, 3H, H<sub>3</sub>), 6.65 (s, 3H, H<sub>4</sub>).



**Scheme S2.** Synthesis of the lanthanide precursors, Ln(tta)<sub>3</sub>(H<sub>2</sub>O)<sub>2</sub> [Ln=La, Eu, Sm, Tb]

## Instruments & physical methods

Infrared spectra of the complexes were recorded in the range 4000-400 cm<sup>-1</sup> with a PerkinElmer FT-IR spectrometer (spectrum two) with the samples following the attenuated total reflectance (ATR) technique. MALDI was performed on a Bruker Daltonics Autoflex Speed MALDI-TOF system (GT0263G201) using *trans*-2-[3-(4-*tert*-Butylphenyl)-2-methyl-2-propenylidene] malononitrile (DCTB) as the matrix. NMR spectra of the compounds were acquired in DMSO-*d*<sub>6</sub> on a Bruker 400 MHz spectrometer using tetramethylsilane (TMS) as an internal standard and

the data were analyzed by Mestre Nova software. Thermogravimetric Analysis (TGA) was executed in a PerkinElmer Thermogravimetric Analyzer (TGA 4000) instrument in a N<sub>2</sub> atmosphere between 30 °C and 800 °C at a heating rate of 10 °C min<sup>-1</sup>. UV-vis absorption spectra of the complexes were recorded with a Shimadzu UV 1800 spectrometer. Steady state luminescence spectra were obtained by a Horiba Fluoromax-4 spectrofluorimeter. Luminescence lifetime measurements were carried out by using time-correlated single photon counting (TCSPC) as well as multi-channel scaling (MCS) set up from Horiba (Deltaflex) and the luminescence decay data were analyzed by using Eztime software. Spectrophotometric titrations and solvatochromic studies were carried out with the compounds having concentration in the order ~10<sup>-5</sup> M. The relative quantum yield at room temperature was measured for all the four complex (**1-4**) in dichloromethane solvent, using quinine sulfate in 1 N H<sub>2</sub>SO<sub>4</sub> ( $\eta = 1.338$ ,  $\Phi = 0.546$ ) as reference for the system. In this regard we have utilized a general equation<sup>S1</sup> for the calculation of quantum yield:

$$\frac{\Phi_s}{\Phi_r} = \frac{A_r \eta_s^2 I_s}{A_s \eta_r^2 I_r}$$

where ‘r’ represents the reference and ‘s’ the sample. ‘A’ implies the absorbance at the excitation wavelength, whereas ‘I’ is the integrated luminescence intensity and ‘ $\eta$ ’ represents the refractive index of the solution. The refractive index is supposed to be equivalent to that of the pure solvent ( $\eta = 1.424$  for dichloromethane). The single-crystal X-ray diffraction data of **5** was collected on a Bruker AXS SMART APEX CCD diffractometer. Data were integrated using CrysAlis<sup>Pro</sup> software with a narrow frame algorithm. Data were subsequently corrected for absorption by the program SCALE3 ABSPACK scaling algorithm. All the structures were solved by the direct methods in SHELLXTL<sup>S2a</sup> and refined by the full-matrix least-squares method on F<sup>2</sup> (SHELXL-2014)<sup>S2b</sup> using the Olex-2 software.<sup>S2c</sup> All the non-hydrogen atoms were refined with anisotropic thermal parameters. All the hydrogen atoms were included in idealized positions, and a riding model was used. All the mean plane analyses and crystallographic Fig.s have been generated using the DIAMOND software (version 3.2k).<sup>S2d</sup> In addition, some disordered solvent molecules were present in complexes **5**. We could not solve the disorder of the solvent molecules properly due to the weak residual Q peaks. So, the Olex-2 mask program was applied to remove the disordered solvent molecules. The possible masked electron counts for void volumes are

calculated as 58, which is assigned to be two acetonitrile (2x19) and two water molecules (2x10). The crystal data and refinement parameters for **5** are summarized in Table S3 and S4.

[Experimental uncertainties are as follows: absorption maxima,  $\pm 2$  nm; molar absorption coefficients, 10%; emission maxima,  $\pm 5$  nm; excited-state lifetimes, 10%; luminescence quantum yields, 20%.]

### FT-IR spectra

IR spectra of the complexes (**1-4**) together with the lanthanide precursors and the ligand tpy-HImzphen were acquired in the solid state to primarily detect the binding of the ligand with the  $\text{Ln}(\text{tta})_3(\text{H}_2\text{O})_2$  precursors and related spectra as well as selected stretching frequencies of the complexes are presented in Fig. S1-S4 and Table S1. The ligand shows a peak at  $\sim 1583 \text{ cm}^{-1}$  due to C=N stretching of the pyridine moieties and a characteristic peak at  $\sim 3180 \text{ cm}^{-1}$  for imidazole N-H stretch. All the lanthanide precursors,  $\text{Ln}(\text{tta})_3(\text{H}_2\text{O})_2$  display a characteristic C=O stretching at  $1601\text{-}1602 \text{ cm}^{-1}$  and a broad hump at  $3351\text{-}3400 \text{ cm}^{-1}$  due to coordinated water molecule. Upon complexation, the C=O stretching frequency moves to  $1605\text{-}1609 \text{ cm}^{-1}$  and the broad peak due to OH stretching within  $3351\text{-}3400 \text{ cm}^{-1}$  of the coordinated water disappeared. Additionally, two new peaks were generated at  $1534\text{-}1538 \text{ cm}^{-1}$  (for C=N stretch) and at  $3080\text{-}3250 \text{ cm}^{-1}$  due to imidazole N-H moiety in the complexes.<sup>32</sup>

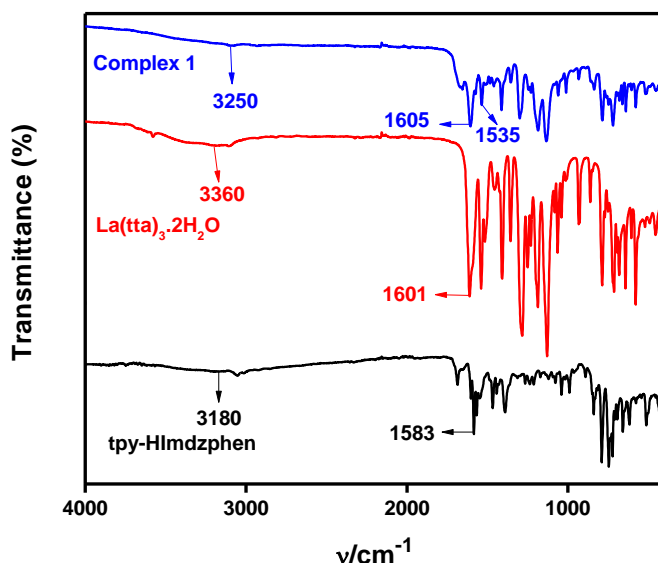


**Fig. S1** FT-IR spectra of tpy-HImzphen,  $\text{La}(\text{tta})_3(\text{H}_2\text{O})_2$  and  $\text{La}(\text{tta})_3\text{tpy-HImzphen}$  (**1**).

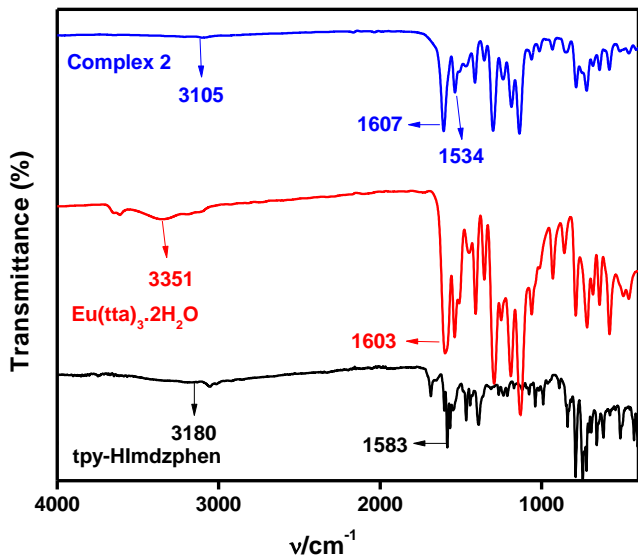


**Fig. S2** FT-IR spectra of tpy-HImzphen, Eu(tta)<sub>3</sub>(H<sub>2</sub>O)<sub>2</sub> and Eu(tta)<sub>3</sub>tpy-HImzphen (**2**).

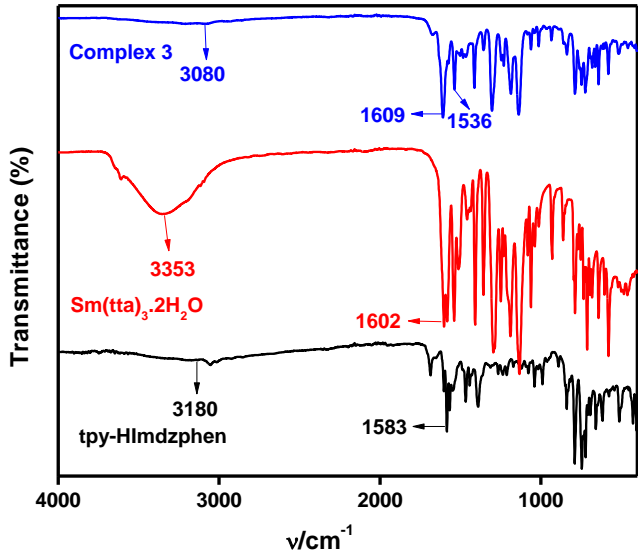


**Fig. S3** FT-IR spectra of tpy-HImzphen, Sm(tta)<sub>3</sub>(H<sub>2</sub>O)<sub>2</sub> and Sm(tta)<sub>3</sub>tpy-HImzphen (**3**).

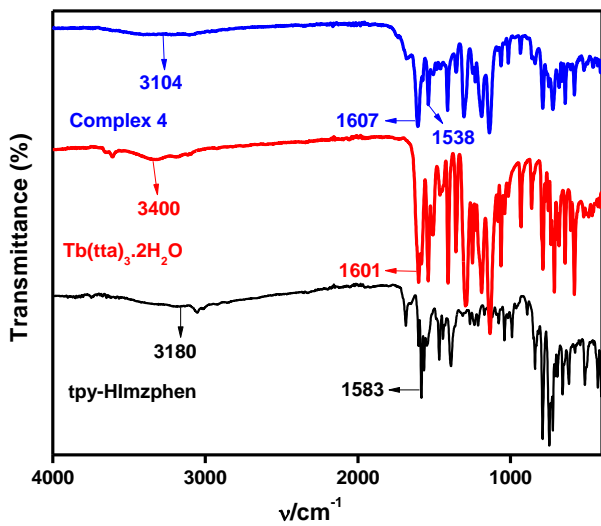


**Fig. S4** FT-IR spectra of tpy-HImzphen, Tb(tta)<sub>3</sub>(H<sub>2</sub>O)<sub>2</sub> and Tb(tta)<sub>3</sub>tpy-HImzphen (**4**).

**Table S1.** Stretching frequencies of selected groups in their FT-IR spectra

Complex:	$\nu_{\text{C=O}}$	$\nu_{\text{C=N}}$	$\nu_{\text{N-H}}$	$\nu_{\text{H}_2\text{O}}$
Tpy-HImdzphen	-	1583	3180	-
La(tta) <sub>3</sub> (H <sub>2</sub> O) <sub>2</sub>	1601	-	-	3360
Complex 1	1605	1535	3250	-
Eu(tta) <sub>3</sub> (H <sub>2</sub> O) <sub>2</sub>	1603	-	-	3351
Complex 2	1607	1534	3105	-
Sm(tta) <sub>3</sub> (H <sub>2</sub> O) <sub>2</sub>	1602	-	-	3353
Complex 3	1609	1536	3080	-
Tb(tta) <sub>3</sub> (H <sub>2</sub> O) <sub>2</sub>	1601	-	-	3400
Complex 4	1607	1538	3104	-

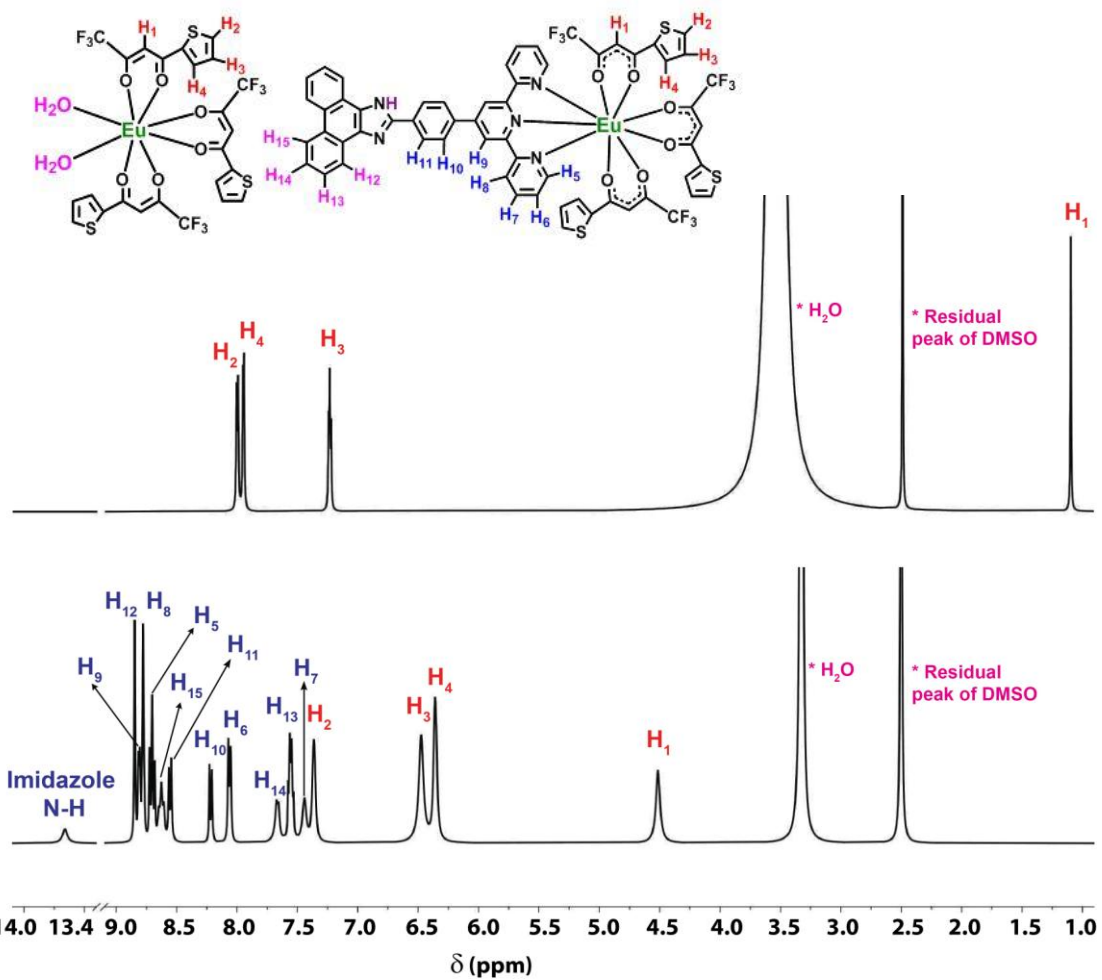


**Fig. S5** 400 MHz  $^1\text{H}$  NMR spectra of  $\text{Eu}(\text{tta})_3(\text{H}_2\text{O})_2$  (top) and  $\text{Eu}(\text{tta})_3(\text{tpy-HImzphen})$  (2) (bottom) in  $\text{DMSO}-d_6$ .

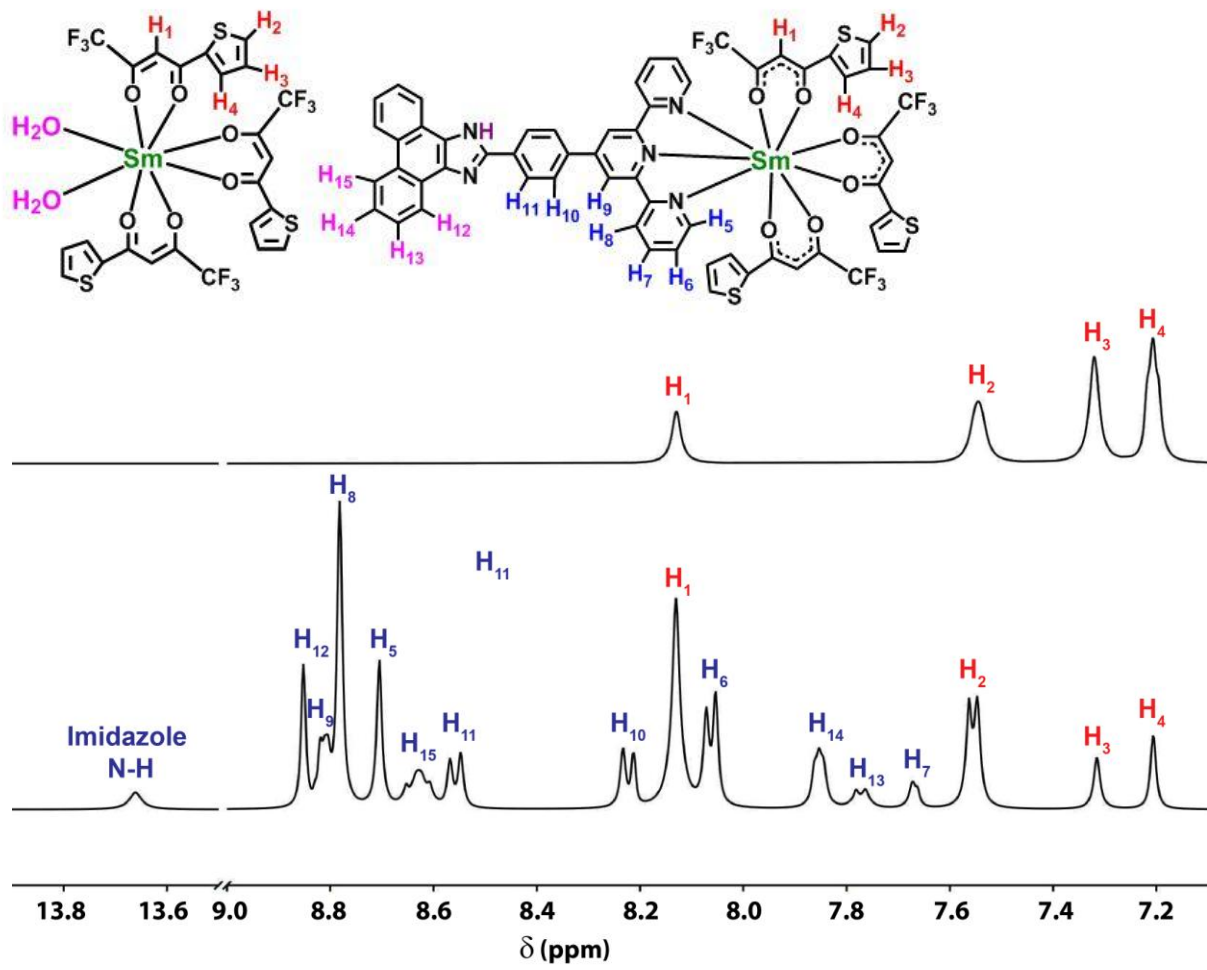


**Fig. S6** 400 MHz  $^1\text{H}$  NMR spectra of  $\text{Sm}(\text{tta})_3(\text{H}_2\text{O})_2$  (top) and  $\text{Sm}(\text{tta})_3(\text{tpy}-\text{HImzphen})$  (3) (bottom) in  $\text{DMSO}-d_6$ .

**Table S2.** Chemical shifts of the protons of all the four complexes in DMSO-*d*<sub>6</sub>.

Proton	Chemical shift (ppm) of Lanthanide complexes ( <b>1-4</b> ) { <i>J</i> = Hz}			
	<b>1</b>	<b>2</b>	<b>3</b>	<b>4</b>
H <sub>1</sub> (methine)	6.18 (s, 3H)	4.51 (s, 3H)	8.13 (s, 3H)	95.20 (s, 3H)
H <sub>2</sub>	~7.80 (m, 3H)	6.36 (s, 3H)	7.55 (t, 3H, <i>J</i> = 6.44 Hz)	29.00 (s, 3H)
H <sub>3</sub>	7.12 (t, 3H, <i>J</i> = 4.0 Hz)	6.48 (s, 3H)	7.32 (s, 3H)	12.16 (s, 3H)
H <sub>4</sub>	~7.80 (m, 3H)	7.36 (s, 3H)	7.21 (s, 3H)	6.58 (s, 3H)
H <sub>5</sub>	8.72 (d, 2H, <i>J</i> = 8.3 Hz)	8.70 (t, 2H, <i>J</i> = 8.0)	8.70 (s, 2H)	8.79 (d, 2H, <i>J</i> = 8.0)
H <sub>6</sub>	8.06 (d, 2H, <i>J</i> = 5.9 Hz)	8.06 (d, 2H, <i>J</i> = 8.0 Hz)	8.06 (d, 2H, <i>J</i> = 8.0 Hz)	8.08 (t, 2H, <i>J</i> = 8.0 Hz)
H <sub>7</sub>	7.56 (t, 2H, <i>J</i> = 6.0 Hz)	7.44 (s, 2H)	7.67 (d, 2H, <i>J</i> = 4.0 Hz)	7.58 (m, 2H)
H <sub>8</sub>	8.81 (d, 2H, <i>J</i> = 5.3 Hz)	8.78 (t, 2H, <i>J</i> = 4.0 Hz)	8.78 (s, 2H)	8.86 (d, 2H, <i>J</i> = 4.52 Hz)
H <sub>9</sub>	8.85 (s, 2H)	8.81 (d, 2H, <i>J</i> = 8.0 Hz)	8.82 (m, 2H)	8.95 (s, 2H)
H <sub>10</sub>	8.22 (d, 2H, <i>J</i> = 7.4 Hz)	8.22 (d, 2H, <i>J</i> = 8.0 Hz)	8.22 (d, 2H, <i>J</i> = 8.0 Hz)	8.32 (d, 2H, <i>J</i> = 8.0 Hz)
H <sub>11</sub>	8.56 (d, 2H, <i>J</i> = 8.3 Hz)	8.55 (d, 2H, <i>J</i> = 8.0 Hz)	8.56 (d, 2H, <i>J</i> = 8.0 Hz)	8.65 (d, 2H, <i>J</i> = 8.0 Hz)
H <sub>12</sub>	8.88 (d, 2H, <i>J</i> = 5.48 Hz)	8.85 (s, 2H)	8.85 (s, 2H)	8.97 (m, 2H)
H <sub>13</sub>	7.67 (d, 2H, <i>J</i> = 8.0 Hz)	7.56 (m, 2H)	7.77 (d, 2H, <i>J</i> = 8.0 Hz)	7.72 (m, 2H)
H <sub>14</sub>	7.74 (d, 2H, <i>J</i> = 8.0 Hz)	7.66 (d, 2H, <i>J</i> = 4.0 Hz)	7.85 (t, 2H, <i>J</i> = 4.0 Hz)	7.84 (m, 2H)
H <sub>15</sub>	8.63 (t, 2H, <i>J</i> = 8.0 Hz)	8.63 (t, 2H, <i>J</i> = 8.0 Hz)	8.63 (t, 2H, <i>J</i> = 8.0 Hz)	8.73 (d, 2H, <i>J</i> = 8.0 Hz)
Imidazole-NH	13.66 (s, 1H)	13.66 (s, 1H)	13.66 (s, 1H)	13.76 (s, 1H)

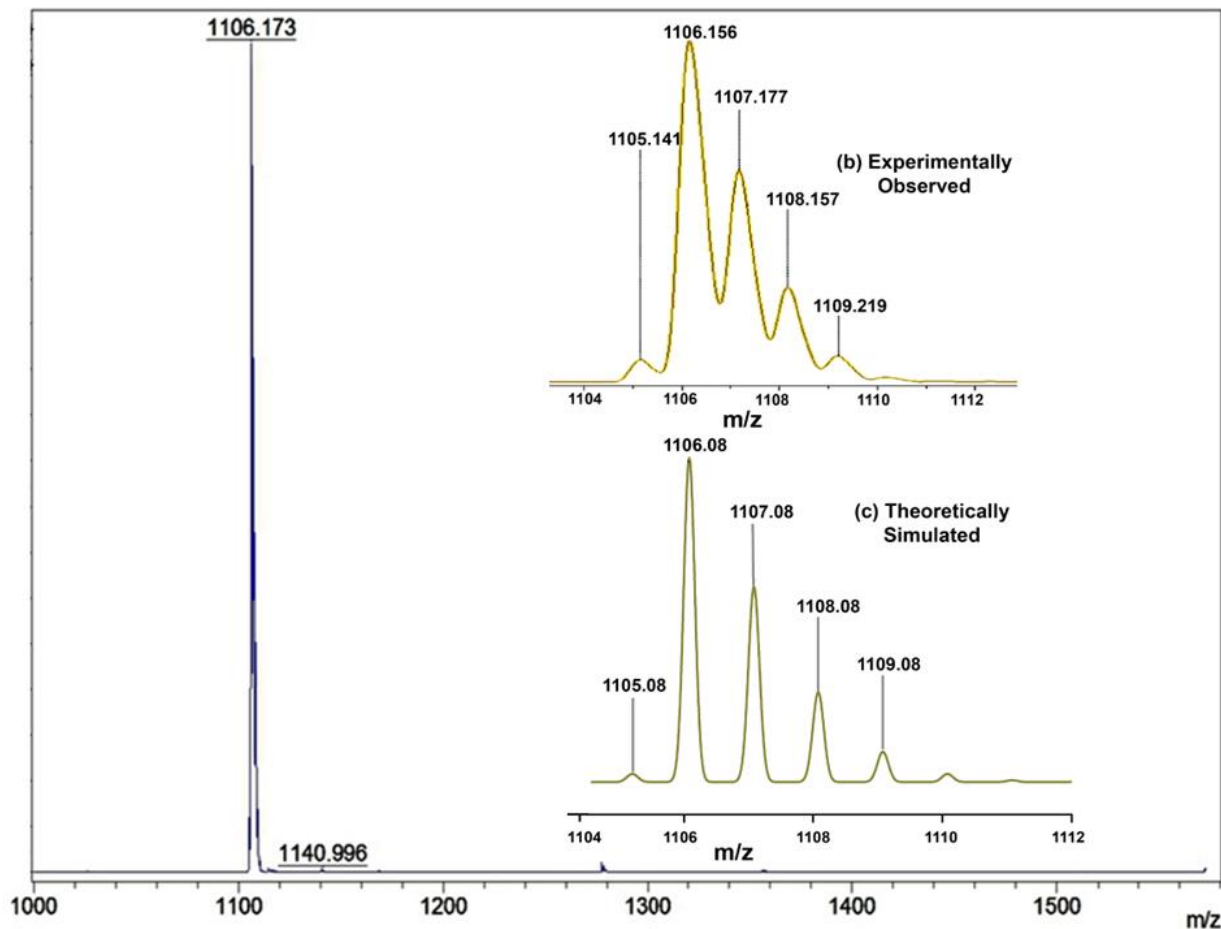


**Fig. S7** MALDI-TOF-MS of  $\text{La}(\text{tta})_3(\text{tpy-HImdzphen})$  (**1**) in dichloromethane solution (positive mode). Upper right portion shows the experimentally observed isotopic distribution pattern (b) and the lower right portion shows the simulated isotopic distribution pattern (c).

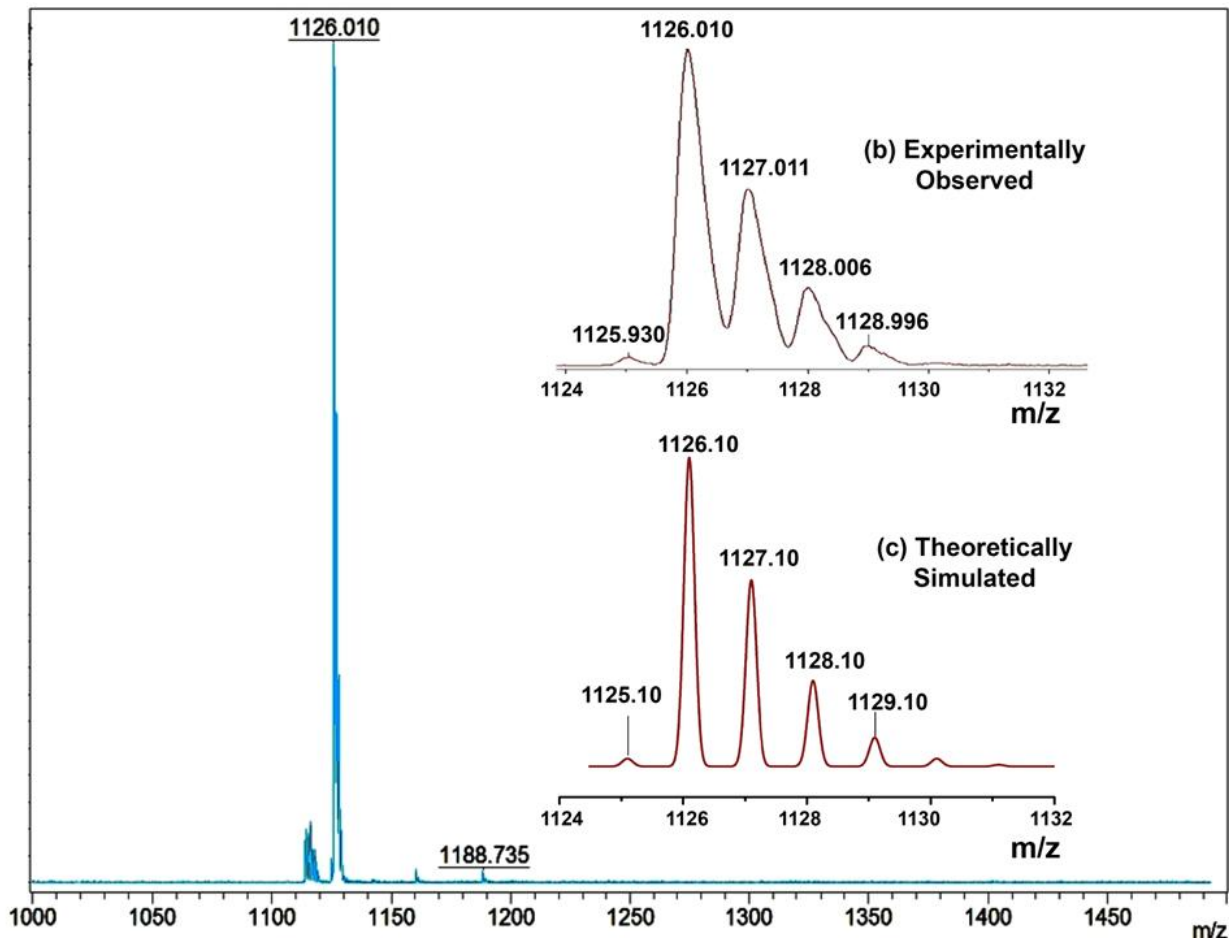


**Fig. S8** MALDI-TOF-MS of  $\text{Tb}(\text{tta})_3(\text{tpy-HImdzphen})$  (**4**) in dichloromethane solution (positive mode). Upper right portion shows the experimentally observed isotopic distribution pattern (b) and the lower right portion shows the simulated isotopic distribution pattern (c).

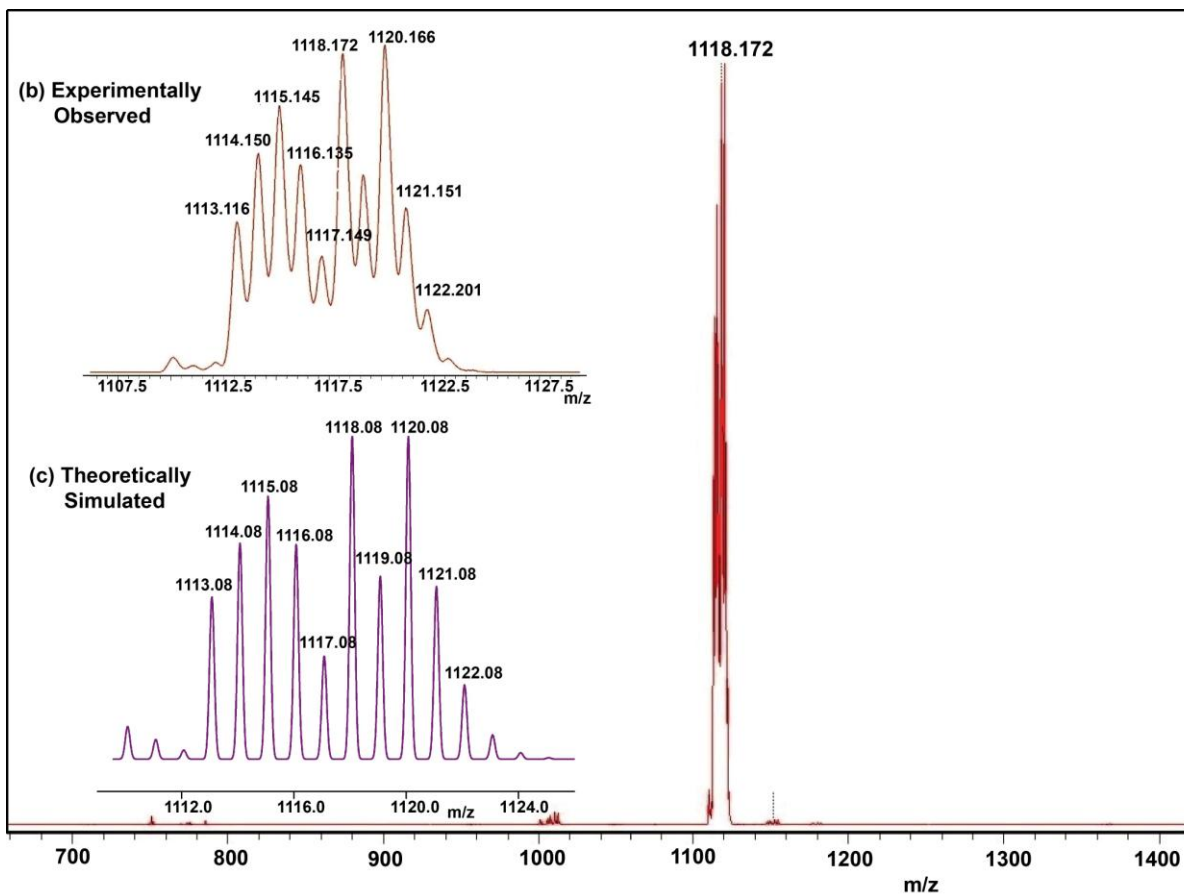


**Fig. S9** MALDI-TOF-MS of  $\text{Sm}(\text{tta})_3(\text{tpy-HImdzphen})$  (**3**) in dichloromethane solution (positive mode). Upper right portion shows the experimentally observed isotopic distribution pattern (b) and the lower right portion shows the simulated isotopic distribution pattern (c).

**Table S3.** Crystallographic parameters for **5**

<b>Compound</b>	<b>5</b>
<b>CCDC Number</b>	2255186
<b>Empirical formula</b>	C <sub>52</sub> H <sub>34</sub> ClF <sub>6</sub> N <sub>5</sub> O <sub>5</sub> S <sub>2</sub> Tb
<b>Formula weight (gmol<sup>-1</sup>)</b>	1181.34
<b>Temperature (K)</b>	108.0
<b>Crystal system</b>	Monoclinic
<b>Space group</b>	C2/c
<b>Unit cell lengths (Å)</b>	a = 10.9321(3) b = 25.1480(7) c = 40.0049(11)
<b>Unit cell angles (°)</b>	α = 90 β = 93.586(2) γ = 90
<b>Volume (Å<sup>3</sup>)</b>	10976.6(5)
<b>Z</b>	8
<b>Density (calculated)</b>	1.430
<b>μ(mm<sup>-1</sup>)</b>	8.086
<b>F(000)</b>	4712.0
<b>Crystal size (mm)</b>	0.16 × 0.12 × 0.09
<b>2θ range for data collection (°)</b>	4.426 to 136.824
<b>Reflections collected</b>	117779
<b>Index ranges</b>	-12 ≤ h ≤ 12, -29 ≤ k ≤ 30, -48 ≤ l ≤ 47
<b>Independent reflections</b>	9791 [Rint = 0.1652, Rsigma = 0.0776]
<b>Data/Restraints/Parameter</b>	9791/13/640
<b>Goodness-of-fit on F<sup>2</sup></b>	1.165
<b>Final R indices [I&gt;2sigma(I)]</b>	R1 = 0.1276, wR2 = 0.2638

**Table S4.** Selected bond angles and bond distances.

Selected Bond distances (Å)		Selected Bond Angles (°)	
Tb1-O4	2.378(8)	O4-Tb1-N2	136.9(3)
Tb1-O3	2.279(7)	O4-Tb1-N1	135.6(3)
Tb1-O5	2.330(9)	O4-Tb1-N3	82.7(3)
Tb1-O2	2.340(8)	O3-Tb1-O4	73.2(3)
Tb1-O1	2.322(9)	O3-Tb1-O5	103.6(3)
Tb1-N3	2.495(9)	O3-Tb1-O2	82.8(3)
Tb1-N2	2.503(8)	O3-Tb1-O1	86.3(3)
Tb1-N1	2.533(10)	O3-Tb1-N2	142.8(3)
		O3-Tb1-N1	78.0(3)
		O3-Tb1-N3	152.3(3)
		O5-Tb1-O4	73.7(3)
		O5-Tb1-O2	140.0(3)
		O5-Tb1-N2	74.4(3)
		O5-Tb1-N1	81.3(3)
		O5-Tb1-N3	81.9(3)
		O2-Tb1-O4	70.6(3)
		O2-Tb1-N2	123.2(3)
		O2-Tb1-N1	137.8(3)
		O2-Tb1-N3	76.4(3)
		O1-Tb1-O4	139.0(3)
		O1-Tb1-O5	146.9(3)
		O1-Tb1-O2	71.8(3)
		O1-Tb1-N2	78.9(3)
		O1-Tb1-N1	69.8(3)
		O1-Tb1-N3	104.0(3)
		N2-Tb1-N1	65.0(3)
		N3-Tb1-N2	64.9(3)
		N3-Tb1-N1	129.7(3)
Hydrogen Bond			
N4-H5B	2.68	N4-H5B-O5	74.83
H5-Cl1	2.29	N5-H5-Cl1	163.55

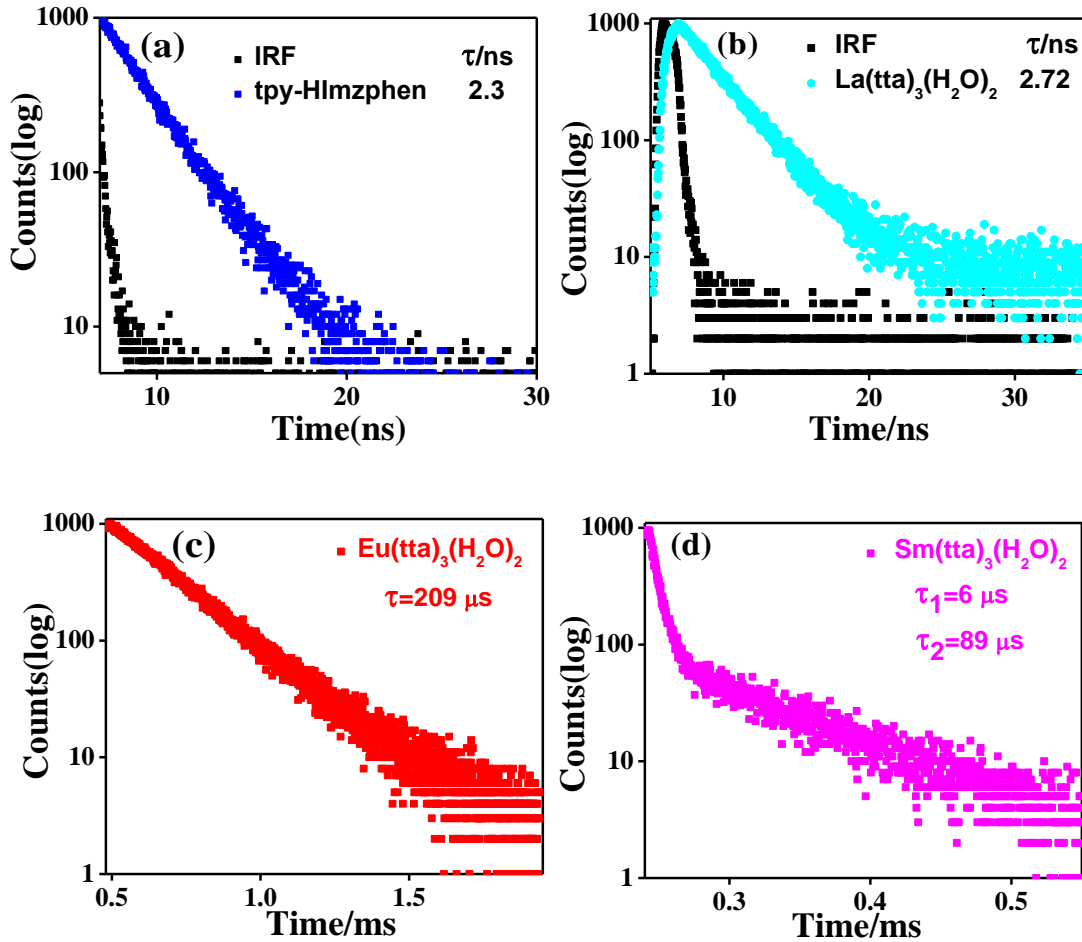


**Fig. S10** Luminescence decay profiles of dichloromethane solution of (a) tpy-HImzphen, (b) La(tta)<sub>3</sub>·2H<sub>2</sub>O, (c) Eu(tta)<sub>3</sub>·2H<sub>2</sub>O and (d) Sm(tta)<sub>3</sub>·2H<sub>2</sub>O, upon excitation at  $\lambda_{\text{exc}}=370\text{nm}$  (insets show the corresponding lifetime values) at RT. [Due to very weak photoluminescence, lifetime decay data could not be collected for Tb(tta)<sub>3</sub>·2H<sub>2</sub>O.]

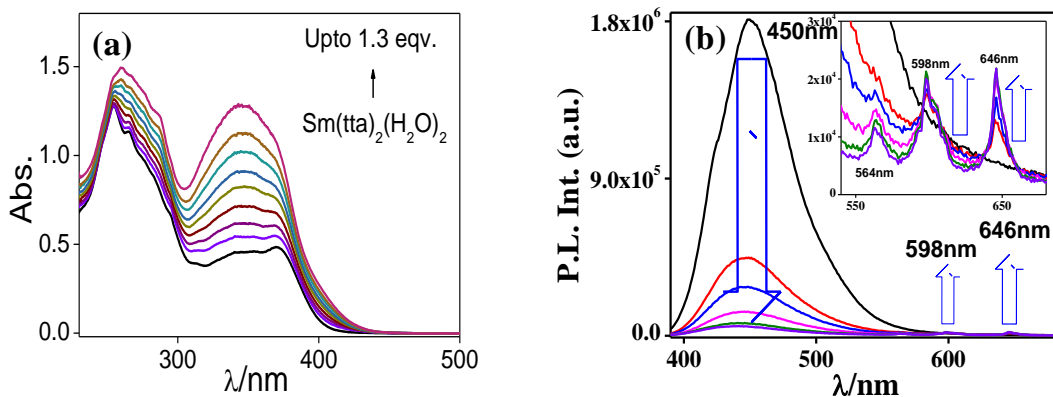


**Fig. S11** Changes in (a) absorption and (b) photoluminescence spectra ( $\lambda_{ex}=370\text{nm}$ ) of ligand tpy-HImzphen upon incremental addition of  $\text{Sm}(\text{tta})_3(\text{H}_2\text{O})_2$  in dry dichloromethane at RT.

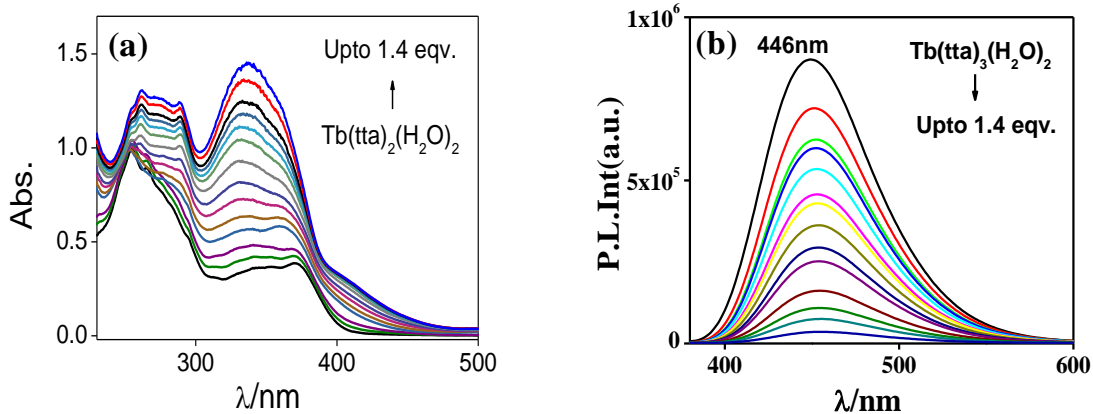


**Fig. S12** Changes in (a) absorption and (b) photoluminescence spectra ( $\lambda_{ex}=370\text{nm}$ ) of ligand tpy-HImzphen upon incremental addition of  $\text{Tb}(\text{tta})_3(\text{H}_2\text{O})_2$  in dry dichloromethane at RT. Inset shows the change of emitting color during titration.

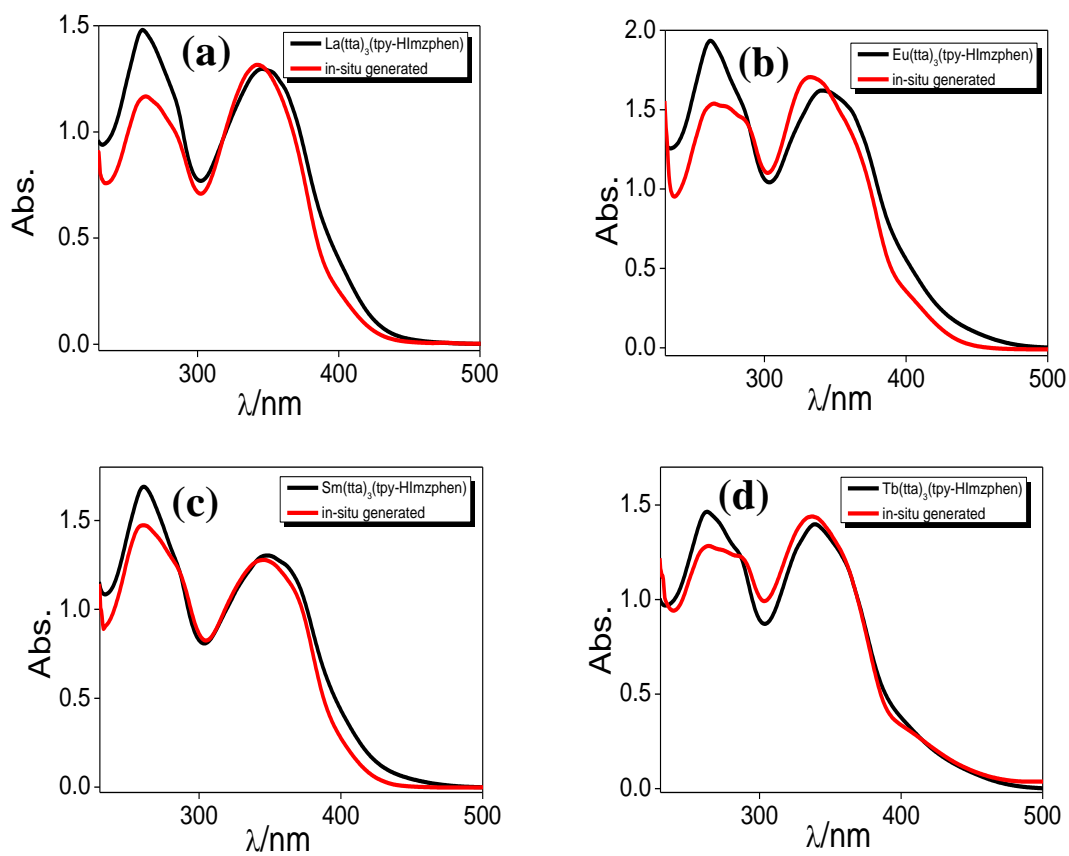


**Fig. S13** Overlayed UV-vis spectra of isolated as well as in-situ generated complex for all four cases: (a) La<sup>III</sup>; (b) Eu<sup>III</sup>; (c) Sm<sup>III</sup>; (d) Tb<sup>III</sup>.

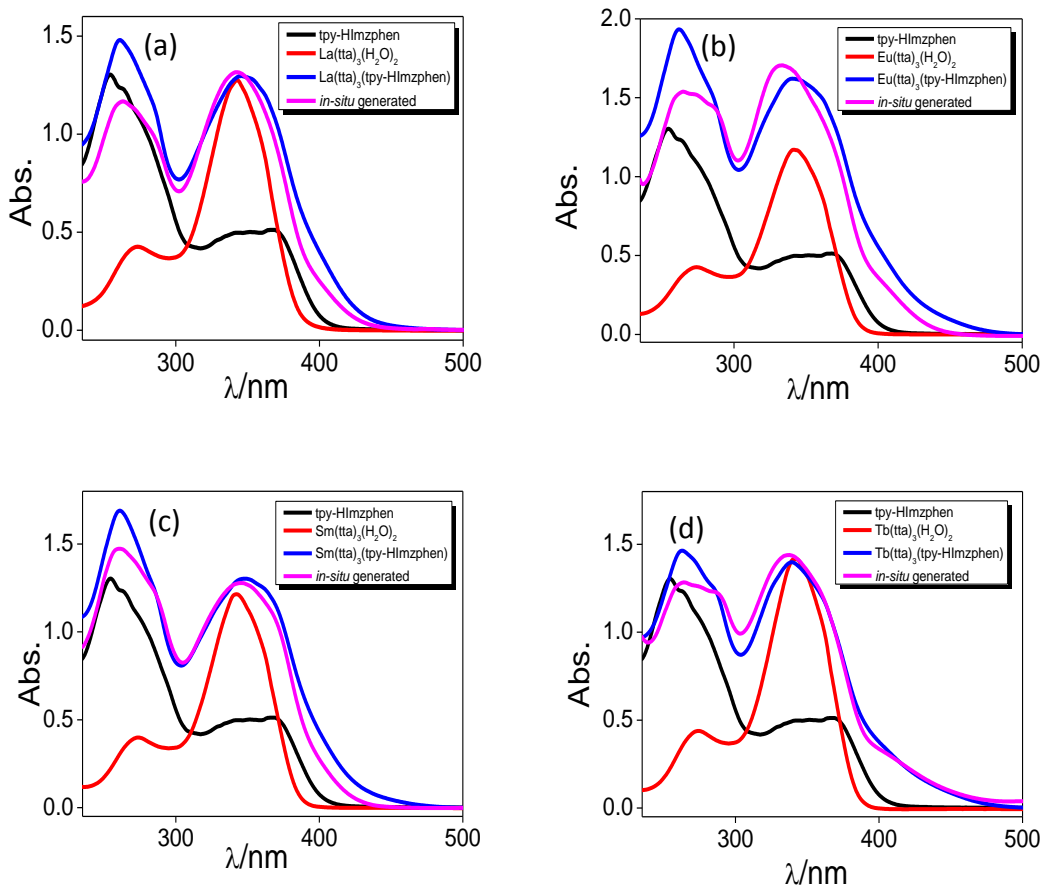


**Fig. S14** Overlayed UV-vis spectra of the chromophore tpy-HImzphen, Ln-tta precursor, isolated complex as well as *in-situ* generated complex for all four cases: (a) La<sup>III</sup>; (b) Eu<sup>III</sup>; (c) Sm<sup>III</sup>; (d) Tb<sup>III</sup>.

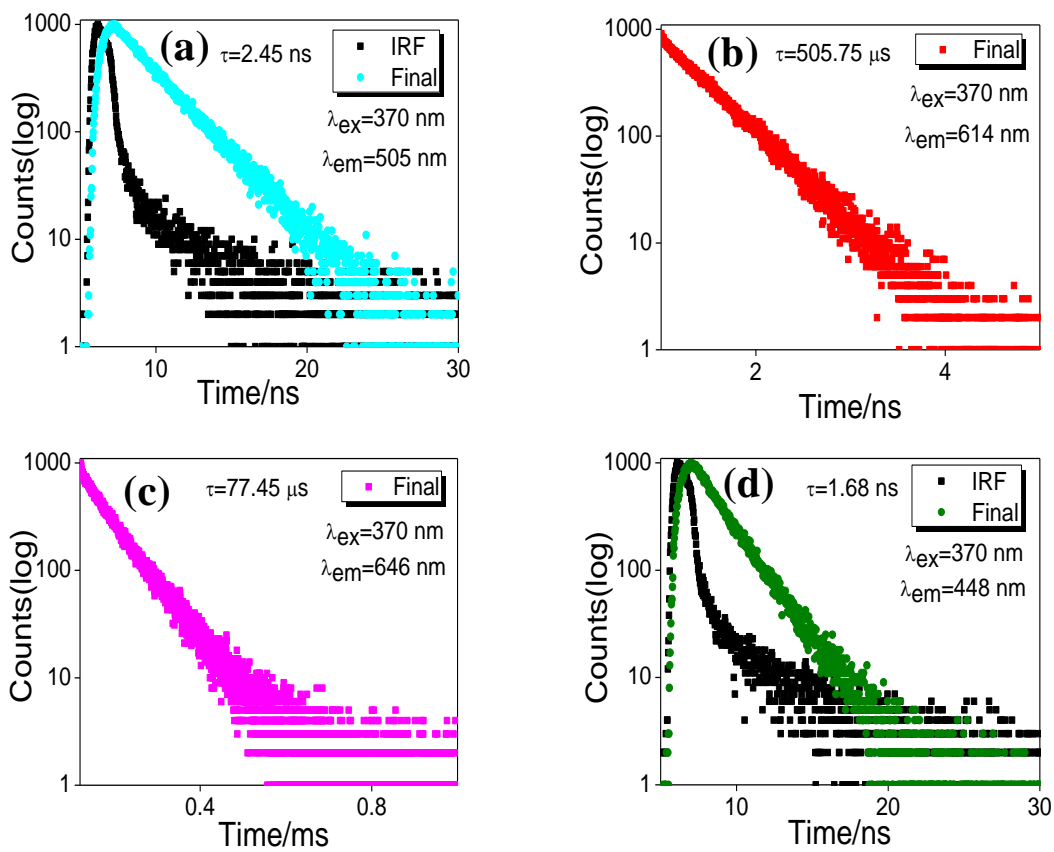


**Fig. S15** Excited state decay profiles at the end of each titration for all four cases: (a)  $\text{La}^{\text{III}}$ ; (b)  $\text{Eu}^{\text{III}}$ ; (c)  $\text{Sm}^{\text{III}}$ ; (d)  $\text{Tb}^{\text{III}}$ .

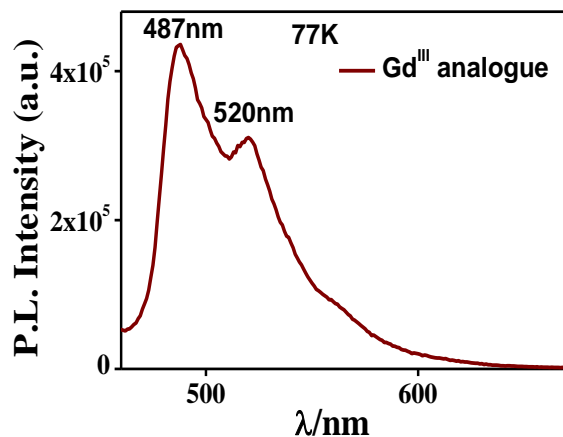


**Fig. S16** Photoluminescence spectrum of  $\text{Gd}^{\text{III}}$ -complex at 77K.

**References:**

- S1. (a) M. Shi, F. Y. Li, T. Yi, D. Q. Zhang, H. M. Hu and C. H. Huang. *Inorg. Chem.*, 2005, **44**, 8929.  
(b) H. Xu, L. H. Wang, X. H. Zhu, K. Yin, G. Y. Zhong, X. Y. Hou and W. Huang. *J. Phys. Chem. B.*, 2006, **110**, 3023.
- S2. (a) *SHELXTL Reference Manual*; Bruker Analytical X-ray Systems, Inc.: W. I. Madison. 2000. (b) G. M. Sheldrick. A short history of SHELX. *Acta Crystallogr., Sect. A: Found. Crystallogr.* 2008, **64**, 112. (c) O. V. Dolomanov, L. J. Bourhis, R. J. Gildea, J. A. K. Howard and H. Puschmann. OLEX2: a complete structure solution, refinement and analysis program. *J. Appl. Crystallogr.* 2009, **42**, 339. (d) K. Bradenburg. *Diamond*, version 3.1 e; Crystal Impact GbR: Bonn, Germany, 2005.